Available online at www.sciencedirect.com
ScienceDirect
Journal of the European Ceramic Society 31 (2011) 2987–2996
www.elsevier.com/locate/jeurceramsoc

Texture development and dielectric relaxor behavior of $0.80Na_{0.5}Bi_{0.5}TiO_3$–$0.20K_{0.5}Bi_{0.5}TiO_3$ ceramics templated by plate-like $NaNbO_3$ particles

Gao Feng *, Liu Liangliang, Xu Bei, Hu GuoXin, Cao Xiao, Hong Rongzi, Tian Changsheng

State Key Laboratory of Solidification Processing, College of Material Science and Engineering, Northwestern Polytechnical University, Xi'an 710072, China

Received 18 January 2011; received in revised form 3 July 2011; accepted 13 July 2011
Available online 5 August 2011

Abstract

Plate-like $NaNbO_3$ particles were used as templates to fabricate grain-oriented $0.96(0.8Na_{0.5}Bi_{0.5}TiO_3$–$0.2\,K_{0.5}Bi_{0.5}TiO_3)$–$0.04NaNbO_3$ (NKBT) ceramics. The effects of the sintering temperature and the soaking time on the grain orientation and the microstructure of the textured NKBT ceramics were investigated, and the dielectric relaxor behavior is discussed. The results show that textured ceramics were successfully obtained with orientation factor more than 0.8. The textured ceramics have a microstructure with strip-like grains aligning in the direction parallel to the casting plane. The degree of grain orientation increases initially, then decreases with increasing sintering temperature, and increases continuously with increasing soaking time. The textured NKBT ceramics shows obvious dielectric relaxor characteristics which can be well explained by microdomain–macrodomain transition theory with calculating criterion K. The results show that formation of texture is beneficial to microdomain–macrodomain transition, which lead to weaken relaxor behavior and raise the dielectric constant at T_{tr}.

Keywords: Perovskites; Tape casting; Grain growth; Texture; Dielectric relaxor

1. Introduction

Recently, the search for lead-free piezoelectric materials replacing $Pb(Ti,Zr)O_3$ (PZT) ceramics has become a very hot topic for the sake of environmental protection. Some lead-free materials have been reported, such as ferroelectric ceramics with perovskite structure, tungsten bronze-type oxides, and Bi-layer structure oxides.[1,2] Among these materials, $Na_{0.5}Bi_{0.5}TiO_3$–$K_{0.5}Bi_{0.5}TiO_3$ ceramics are receiving greater attention. The morphotropic phase boundary (MPB) of $(1-x)Na_{0.5}Bi_{0.5}TiO_3$–$xK_{0.5}Bi_{0.5}TiO_3$ system exists in the range of $x = 0.16$–0.20 with relative high piezoelectric properties.[3,4] But compared with the conventional PZT piezoelectric ceramics, $Na_{0.5}Bi_{0.5}TiO_3$–$K_{0.5}Bi_{0.5}TiO_3$ ceramics still show poor piezoelectric properties, which have restricted the applications of the material. To further improve its piezoelectric properties, attempts of doping different valence ions and combining new compound with $Na_{0.5}Bi_{0.5}TiO_3$–$K_{0.5}Bi_{0.5}TiO_3$ to form multi-component solid solution has been extensively studied.[5–7] But the results are not desirable.

Currently it is reported that the method of controlling microstructure with grain orientation makes it possible to obtain ceramic materials with the desired properties.[2,8,9] As an alternative to techniques such as hot pressing and hot forging, reactive-templated grain growth (RTGG) offers the possibility of fabricating grain-oriented polycrystalline ceramics. In this method, template particles must be large and anisometric in shape, so that they can be oriented during tape casting and grown preferentially during sintering stage.[10–12] The best material for seeding the phase formation of $Na_{0.5}Bi_{0.5}TiO_3$–$K_{0.5}Bi_{0.5}TiO_3$ and to template its oriented growth would be $Na_{0.5}Bi_{0.5}TiO_3$ or $K_{0.5}Bi_{0.5}TiO_3$. However, anisotropically shaped $Na_{0.5}Bi_{0.5}TiO_3$ and $K_{0.5}Bi_{0.5}TiO_3$ particles are difficult to prepare. Some particles with anisometric in shape such as TiO_2, $SrTiO_3$, $Bi_4Ti_3O_{12}$, $SrBi_4Ti_4O_{15}$, and Al_2O_3 have been used as template to fabricated textured lead free piezoelectric ceramics.[13–16]

$NaNbO_3$, another important lead free piezoelectric compound, demonstrates orthorhombic symmetry and an

* Corresponding author.
E-mail address: gaofeng@nwpu.edu.cn (F. Gao).

0955-2219/$ – see front matter © 2011 Elsevier Ltd. All rights reserved.
doi:10.1016/j.jeurceramsoc.2011.07.018

anti-ferroelectric response at room temperature.[17] What is more, the lattice structure of $NaNbO_3$ has a perovskite cell, which is similar to the perovskite crystal structure of $Na_{0.5}Bi_{0.5}TiO_3$–$K_{0.5}Bi_{0.5}TiO_3$. If plate-like $NaNbO_3$ can be prepared and be used as template particles, it will result in good extension grain growth relationship. However, research on $Na_{0.5}Bi_{0.5}TiO_3$–$K_{0.5}Bi_{0.5}TiO_3$ solid solution by RTGG method using $NaNbO_3$ as template particles has rarely been reported.

In our previous study, the effects of plate-like $NaNbO_3$ content on the microstructure and properties of non-textured $0.8Na_{0.5}Bi_{0.5}TiO_3$–$0.2\,K_{0.5}Bi_{0.5}TiO_3$ ceramics were investigated. The optimal content of $NaNbO_3$ for textured ceramic template was 4 mol%.[18] In the present study, plate-like $NaNbO_3$ (NN) template particles were synthesized by the two-step NaCl–KCl molten salt process, and textured $0.96(0.8Na_{0.5}Bi_{0.5}TiO_3$–$0.2\,K_{0.5}Bi_{0.5}TiO_3)$–$0.04NaNbO_3$ ceramics were fabricated by RTGG in combination with tape casting. The effects of sintering conditions on the phase structure, the grain orientation and the dielectric relaxor behavior were investigated.

2. Experimental procedure

2.1. Preparation of plate-like $NaNbO_3$ templates

Plate-like $NaNbO_3$ (NN) template particles were prepared by two-step NaCl–KCl molten salt synthesis (MSS).[19] Reagent-grade Bi_2O_3, Na_2CO_3, Nb_2O_5, NaCl, and KCl were used as starting materials. Firstly, bismuth layer-structured plate-like $Bi_{2.5}Na_{3.5}Nb_5O_{18}$ (BNN) particles with an average diameter of ~5 μm and a thickness of 1 μm are synthesized by the MSS method.[20] Secondly, using plate-like BNN as precursor, plate-like $NaNbO_3$ particles are synthesized through a chemical reaction, as shown in Eq. (1):

$$4Bi_{2.5}Na_{3.5}Nb_5O_{18} + 3Na_2CO_3 \rightarrow 20NaNbO_3 + 5Bi_2O_3 + 3CO_2\uparrow \quad (1)$$

The starting materials plate-like $Bi_{2.5}Na_{3.5}Nb_5O_{18}$ and Na_2CO_3 (99%) were weighed in Na_2CO_3/BNN weight ratios of 1.50:1, then an equal weight of NaCl–KCl mixture was added to them. They were mixed by ball-milling in ethanol for 12 h and calcined in a sealed alumina crucible at 950 °C for 8 h. After slowly cooling to room temperature, the reaction product was washed ~10 times with hot de-ionized water and the NN template was separated by using HNO_3 to remove the by-product Bi_2O_3. Then the powder was rewashed ~20 times with hot de-ionized water until no free Cl^- ions were detected using $AgNO_3$ solution. The NN templates were obtained by drying at 80 °C for 10 h. As shown in Fig. 1, no other new phase is detected and pure NN phase was obtained. The NN powder is formed of plate-like particles with an average diameter of 5–10 μm and a thickness of 1–2 μm, which can meet the needs of the RTGG method.

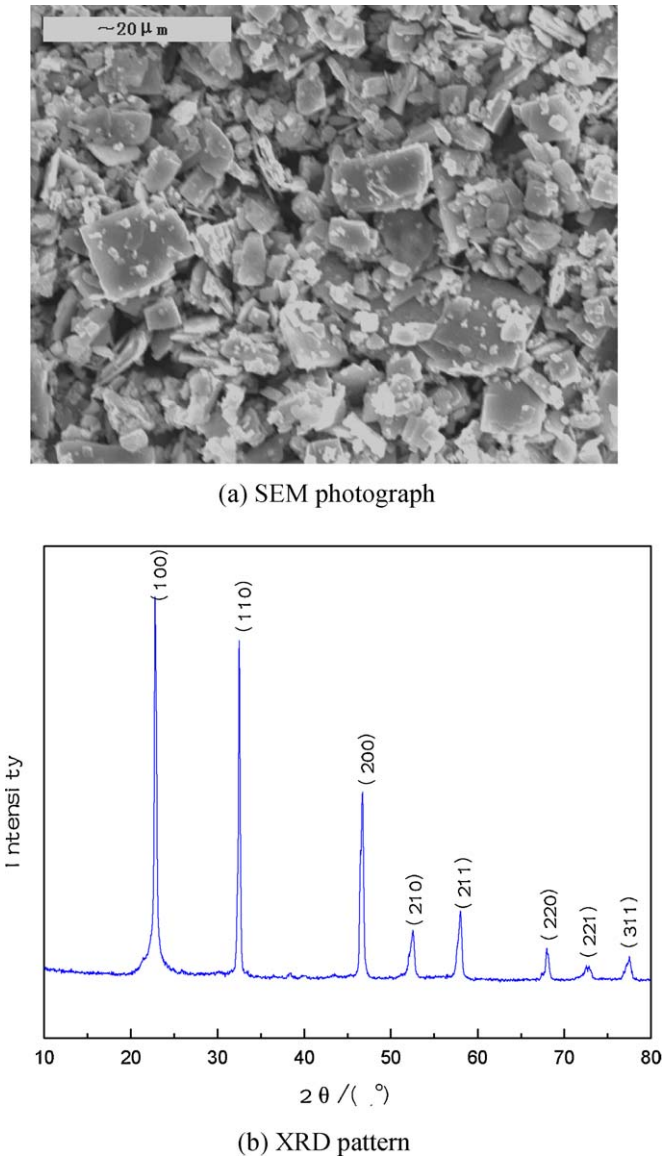

(a) SEM photograph

(b) XRD pattern

Fig. 1. SEM photograph and XRD pattern of $NaNbO_3$ template particles: (a) SEM photograph and (b) XRD pattern.

2.2. Fabrication of textured NKBT ceramics by RTGG

The general formula of the material studied was $0.96(0.8Na_{0.5}Bi_{0.5}TiO_3$–$0.2\,K_{0.5}Bi_{0.5}TiO_3)$–$0.04NaNbO_3$ (abbreviated as NKBT). The samples were prepared by RTGG in combination with tape casting. Before weighed the raw materials, Bi_2O_3, TiO_2, Na_2CO_3, and K_2CO_3 powders were baked at 120 °C for 4 h to eliminate humidity of powders. Reagent-grade Bi_2O_3, TiO_2, Na_2CO_3, K_2CO_3 powders and solvent, binder, plasticizer were mixed and ball milled for 48 h. The solvents were ethanol and xylene. The binder and plasticizer were polyvinyl alcohol (PVA) and glycerin, respectively. After completion of the ball milling process on the slurry, 4 mol% plate-like NN template particles were added and mixed with the slurry for 4 h. Then the slurry was degassed under vacuum and tape cast on a plated steel surface with a blade gap of 100 μm. The green tapes were cut into pieces of 100 mm × 100 mm

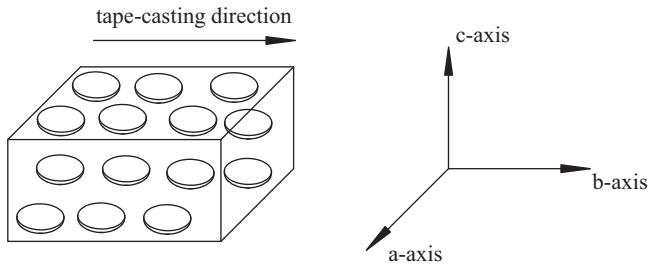

Fig. 2. The sketch map of textured NKBT ceramics by RTGG method.

and laminated at a pressure of 100 MPa for 15 min. After the laminated samples were cut into 10 mm × 10 mm squares, the binder and plasticizer were burned out at 500 °C for 2 h with a heating rate of 1 °C/min. Then the samples were sintered at 1100–1200 °C for 2–10 h. Sections, as shown in Fig. 2, were polished perpendicular (a–c plane) to the tape-casting direction, to discuss the texture development. What is more, the sintered ceramics were painted with silver on both surface parallel (a and b plane) to the tape-casting direction.

2.3. Microstructure characterization

The crystal structure and grain orientation were determined by the intensity of X-ray diffraction (XRD; model Panalytical X'Pert PRO, Holland) on the major surfaces of sintered ceramics, with 2θ in the range of 20–70° and with a step of 0.02°. The microstructure was observed by scanning electron microscopy (SEM; Model Hitachi S-570, Japan) on polished surfaces perpendicular to the tape casting direction. The temperature dependence of dielectric constant (ε) and dielectric loss ($\tan\delta$) were measured between 30 °C and 450 °C using an HP4284 LCR precision electric bridge.

3. Results and discussions

3.1. Microstructure of textured NKBT ceramics

Non-textured NKBT ceramics with adding 4 mol% plate-like NN particles were prepared by traditional process and X-ray diffraction (XRD) was performed after samples were sintered at 1130, 1150, 1170, and 1200 °C. Fig. 3 shows XRD patterns of non-textured and textured NKBT ceramics. As shown in Fig. 3(a), there are two phases coexist in the ceramics, one is NKBT with perovskite structure, and the other is $K_2Ti_8O_{17}$ phase. From Fig. 3(b), it can be seen that the same phases, NKBT and $K_2Ti_8O_{17}$ phase, coexist in the textured ceramics. The content of $K_2Ti_8O_{17}$ phase, which is resulted from the raw materials K_2CO_3 and TiO_2, has little change. That no peak of NN appeared means that the NN templates react with the original powder to form texture grains. The (1 1 0) peak is the main intense peak in the non-textured NKBT ceramics with randomly oriented grains. While the intensity of the (2 0 0) peak increases, and the whole trend of (1 1 0) intensity is become smaller as the sintering temperature rising. The results indicate that (h 0 0) texture is formed in the NKBT ceramics prepared by RTGG. The

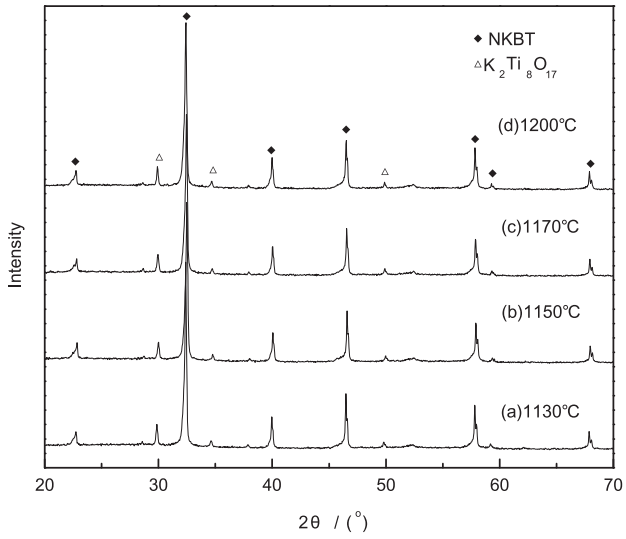

(a) non-textured NKBT ceramics

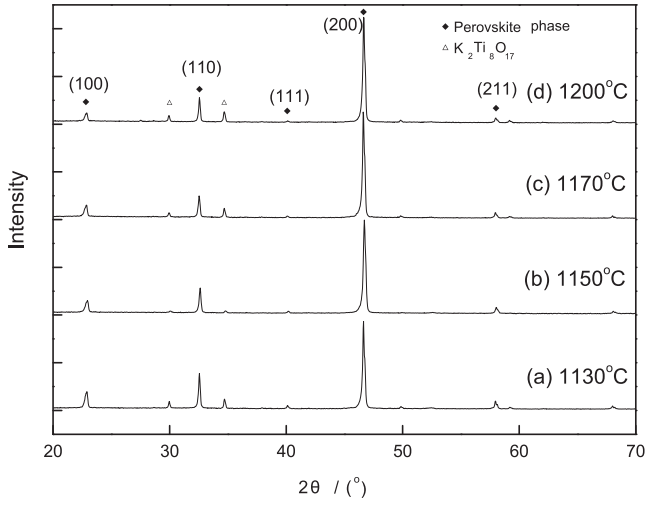

(b) textured NKBT ceramics

Fig. 3. XRD patterns of non-textured and textured NKBT ceramics sintered at different temperatures: (a) non-textured NKBT ceramics and (b) textured NKBT ceramics.

texture fraction (f) is calculated by the Lotgering method, as the following equations show:[21]

$$f = \frac{P - P_0}{1 - P_0} \tag{2}$$

$$P = \frac{\sum I_{\{h\ 0\,0\}}}{\sum I_{\{h\,k\,l\}}} \tag{3}$$

$$P_0 = \frac{\sum I_{0\{h\,0\,0\}}}{\sum I_{0\{h\,k\,l\}}} \tag{4}$$

where I and I_0 are the peak intensities of the sintered compacts and randomly oriented NBTBT, respectively. $\{h\,0\,0\}$ and $\{h\,k\,l\}$ are Miller indexes. The diffraction lines between $2\theta = 20°$ and $2\theta = 70°$ are used to calculate P and P_0.

Fig. 4 shows the effect of sintering temperature on the degree of orientation for NKBT ceramics. The degree of orientation

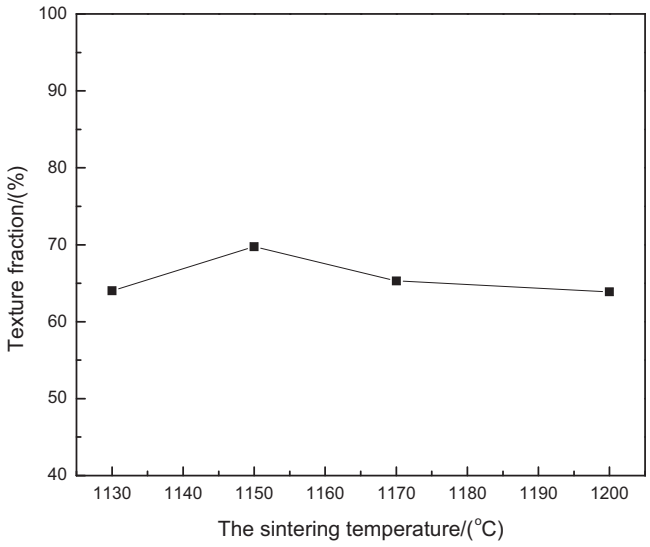

Fig. 4. Texture fraction of NKBT textured ceramics sintered at different temperatures.

Table 1
Densities of the textured NKBT ceramics sintered at different temperatures.

Sintering temperature (°C)	1130	1150	1170	1200
Density (g/cm^3)	5.525	5.643	5.598	5.578
Relative density (%)	93.2	95.2	94.4	94.1

was 0.64 in the samples sintered at 1130 °C. But f increases as the sintering temperature increases and the largest volume (0.70) is present at 1150 °C. A more textured material is present with increasing sintering temperature from 1130 °C to 1150 °C, and NKBT ceramics sintered at 1150 °C have significant grain orientation.

The densities of the ceramics were measured by the Archimedes method. The theory densities of $Na_{0.5}Bi_{0.5}TiO_3$, $K_{0.5}Bi_{0.5}TiO_3$, and $NaNbO_3$, which is gotten from standard XRD card, are 5.997 g/cm^3 (No. 36-0340), 5.929 g/cm^3 (No. 36-0339), and 4.60 g/cm^3 (No. 74-2458), respectively. So the theory density of $0.96(0.8Na_{0.5}Bi_{0.5}TiO_3–0.2\,K_{0.5}Bi_{0.5}TiO_3)–0.04NaNbO_3$ is 5.928 g/cm^3. Table 1 shows the change in the measured density of the NKBT ceramics as a function of sintering temperature. It was found that all the textured NKBT ceramics

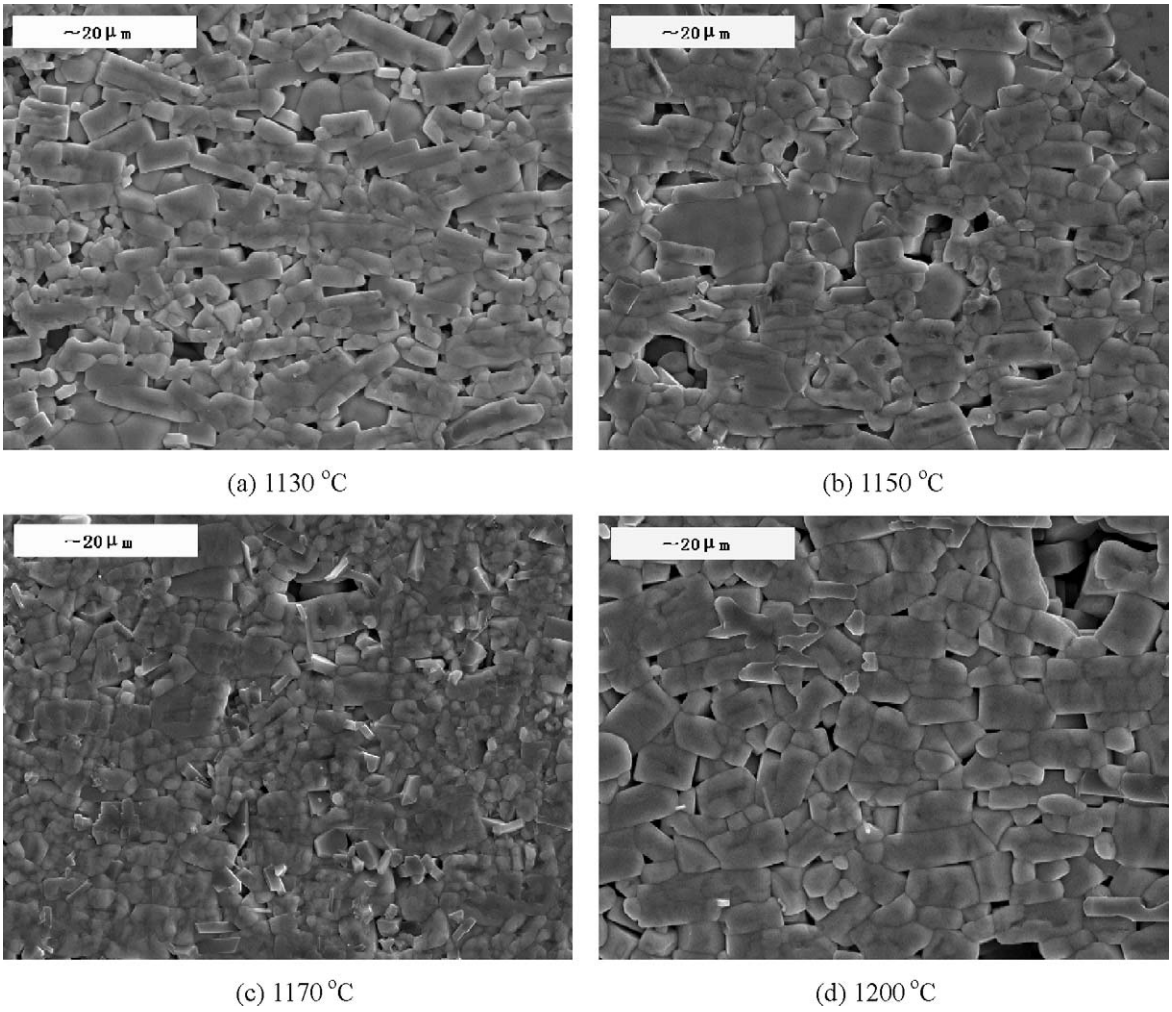

Fig. 5. Microstructure of NKBT textured ceramics sintered at different temperatures: (a) 1130 °C, (b) 1150 °C, (c) 1170 °C and (d) 1200 °C.

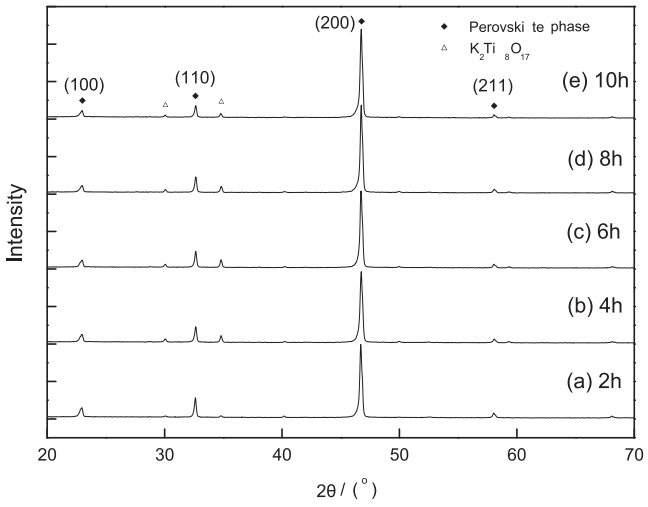

Fig. 6. XRD patterns of NKBT textured ceramics with different soaking times.

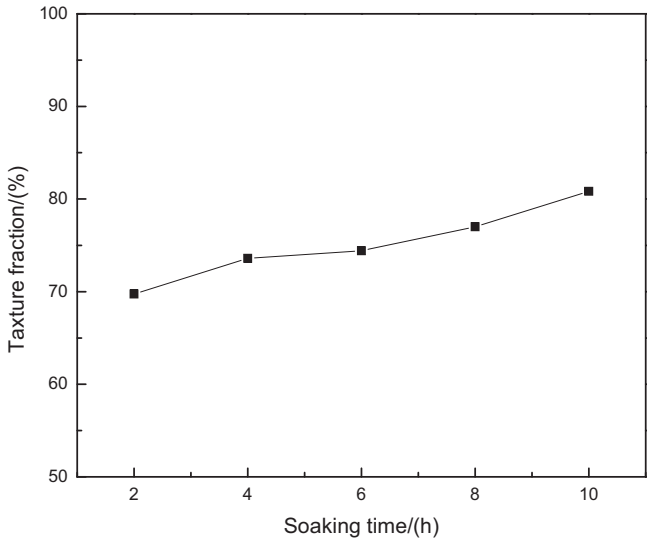

Fig. 7. Texture fraction of NKBT textured ceramics with different soaking times.

have relative densities higher than 93%, which means that the ceramics have achieved good densification under the experimental conditions used. The density increases from 5.525 to 5.643 g/cm^3. When the sintering temperature is higher than 1150 °C, the density decreases. The maximum relative density, 95.2%, is achieved at 1150 °C. The density of the non-textured NKBT ceramics sintered at 1150 °C for 2 h is 5.667 g/cm^3. So textured NKBT ceramics have the same composition, the same phase structure, and comparable densities with the non-textured NKBT ceramics.

Fig. 5 shows the microstructure of NKBT ceramics with polished plane perpendicular to the tape casting direction (a–c plane). All specimens are composed of two types of NKBT grains. One is a strip-like grain, which originates from plate-like NN particles. It can be seen that the plate face is parallel to the casting plane, and the thickness is larger than that of the original NN templates. The other is a fine, equiaxed shaped grain. These two grain types are called oriented and matrix grains, respectively. It is clear that the thickness of the oriented grains increases as the sintering temperature increases. The matrix grains also grow and their shapes change to cubic. The size and uniformity of the grains are clearly seen with increasing temperature, and at the same time, the grains grow with apparent orientation. It is found that a brick-wall microstructure with grain size up to ~15 μm in length and ~5 μm in thickness was obtained in the NKBT ceramics sintered at 1200 °C.

Fig. 6 shows XRD patterns of NKBT textured ceramics sintered at 1150 °C with different soaking times. It is seen that NKBT and $K_2Ti_8O_{17}$ phases coexist in the ceramics. The (2 0 0) peak is the main intense peak in the ceramics. Although an 10 h soaking time is longer enough, $K_2Ti_8O_{17}$ phase is still alive. The results show that increasing the soaking time cannot eliminate the $K_2Ti_8O_{17}$ phase. Fig. 7 shows the effect of soaking time on the degree of orientation of NKBT ceramics. The texture fraction increases as the soaking time increases and the maximum is 0.81 at 10 h. Table 2 shows densities of the textured NKBT ceramics sintered at different soaking time. It was found that the density increases firstly. When the soaking time is longer than 6 h, the density decreases slightly. It should be resulted from the evaporation of Bi, Na, and K at high temperature. The maximum relative density, 96.1%, is achieved at 1150 °C sintered for 6 h.

Fig. 8 shows SEM micrographs of NKBT textured ceramics with different soaking times. It is revealed that the grains with almost square shape grow larger and larger with extending soaking time. At the same time, some abnormal grain growths are observed. A number of the huge cubic grains with the size of 20 μm in length and 8–10 μm in thickness were obtained in the NKBT ceramics sintered at 10 h, as shown in Fig. 8(d).

Our previously research work from grain growth kinetics demonstrated that the crystal formation of textured $Na_{0.5}Bi_{0.5}TiO_3$–$BaTiO_3$ ceramics with plate-like $Bi_{2.5}Na_{3.5}Nb_5O_{18}$ templates is a diffusion—recrystallization process.[20] The grain growth mechanism of oriented grains is controlled by grain lattice diffusion and grain boundary diffusion. Because of the similarity between the crystal structure of $Na_{0.5}Bi_{0.5}TiO_3$–$BaTiO_3$ and NKBT, the mechanism of the grain orientation is the same pattern. That once two-dimensional nucleation has formed on the NN crystal surface, the crystal will grow along the interface. The texture fraction increases with the growth of the oriented grains and the effect on the adjacent grains, finally brick-wall morphology is obtained.

3.2. Dielectric relaxor behavior of textured NKBT ceramics

Fig. 9 shows the dielectric properties of textured and non-textured NKBT ceramics as a function of temperature at different frequencies. As Fig. 9(a) shown, the non-textured NKBT ceramics show evidence of diffuse phase transition, which is typical for relaxor ferroelectrics. It can be seen that ε increases with

Table 2
Densities of the textured NKBT ceramics sintered at different soaking times.

Soaking time (h)	4	6	8	10
Density (g/cm^3)	5.679	5.697	5.621	5.554
Relative density (%)	95.8	96.1	94.8	93.7

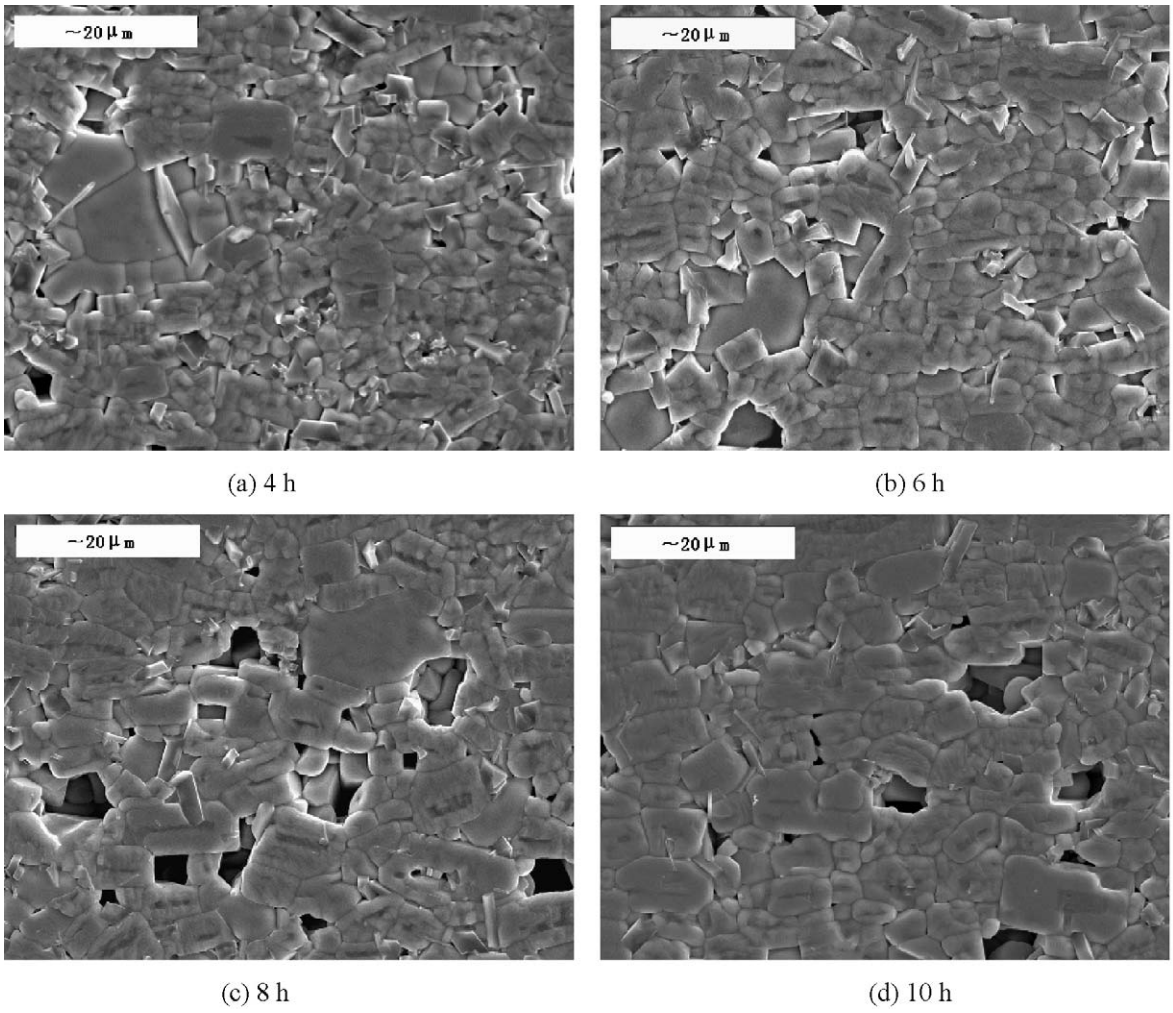

Fig. 8. SEM micrographs of NKBT textured ceramics with different soaking times: (a) 4 h, (b) 6 h, (c) 8 h and (d) 10 h.

increasing temperature and reveals a transition temperature T_{tr} of around ~95 °C and "a maximum temperature" T_m of about 304 °C. The two temperatures correspond to induced phase transitions. The first one is at ~95 °C between rhombohedral ferroelectric (*R*3*C*) and a tetragonal phase, and the second one is at ~304 °C between the tetragonal ferroelectrics and cubic paraelectric phases. In the same figure, the dielectric loss is also given as a function of temperature. That the dielectric loss peaks located around the first transition temperature was given as a proof for the phase transition from rhombohedral to tetragonal.

In the previous reports, T_m stands for the temperature corresponding to the maximum value of dielectric constant which is also called the Curie temperature, and ε at T_{tr} is much smaller than ε at T_m. In the present study, Fig. 9(b) shows that T_m of the textured NKBT ceramic was not "a maximum temperature" but a transition temperature from a tetragonal ferroelectric to a paraelectric state, because the dielectric constant at T_{tr} is obviously higher than that of T_m. The maximum dielectric constant measured for the non-textured NKBT ceramics was 1000 and 1580 at T_{tr} and T_m, respectively, whereas those for the textured ceramics was 1490 and 1250. Besides diffuse phase transition, a strong frequency dispersion of the dielectric constant is clearly seen for the textured NKBT ceramic. The dielectric constant decreased and its maximum at T_{tr} shifted to higher temperatures as the measurement frequency increases.

The two interesting results should be discussed. Firstly, it is obviously that the relaxor behavior of the non-textured NKBT ceramic is stronger than that of the textured NKBT ceramic. Secondly, it is clear that the dielectric constant at T_{tr} is obviously higher than that of T_m for the textured NKBT ceramics.

The relaxor behavior originated from the composition fluctuations in site occupancy.[22] It has been demonstrated that three states, macrodomain, microdomain and polar micro region, will appear in the ferroelectric ceramics with the increasing of temperature. The microdomain–macrodomain transition is a quantum transition process, while the driving forces are mainly heating force and energy force. The stability of microdomain–macrodomain transition can be judged by both the activating energy and state parameter. According to Gaussian distribution equation, the function of the amount of microdomain (N) and the Curie temperature (T_m) can be expressed as the following equation:[23]

$$N = N_0 \exp\left[-\frac{(T - T_m)^2}{2\delta^2}\right] \quad (5)$$

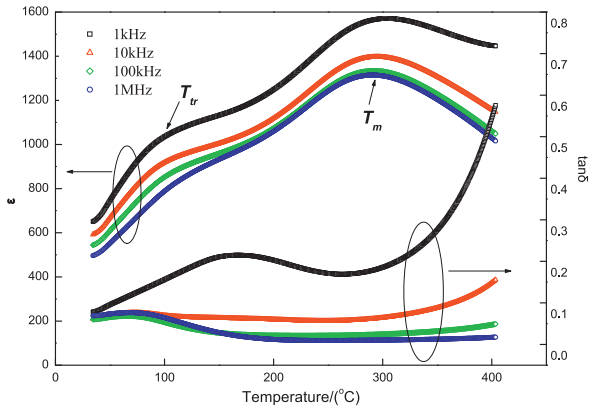

(a) non-textured NKBT ceramics

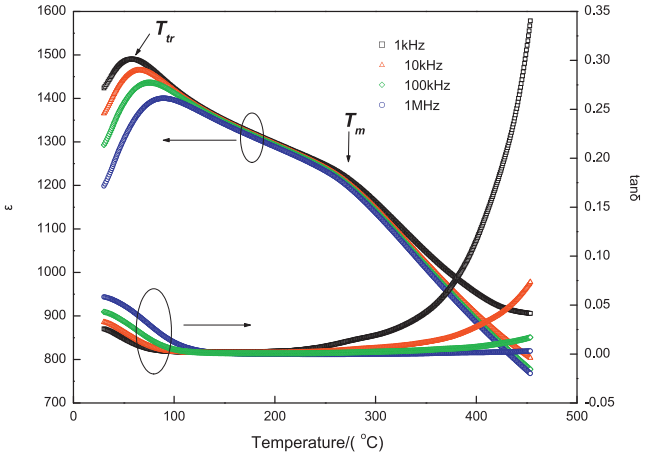

(b) textured NKBT ceramics

Fig. 9. The dielectric properties as a function of temperature for (a) non-textured NKBT ceramics and (b) textured NKBT ceramics.

where N_0 is the total number of the polar micro regions, and δ is the degree of diffusion phase transition. Then the volume percentage of microdomain (φ) can be calculated with arranging Eq. (5):

$$\varphi = \frac{N}{N_0} = \exp\left[-\frac{(T - T_m)^2}{2\delta^2}\right] \tag{6}$$

From Eq. (6), it can be deduced that the main factors influencing φ are T_m and δ. For NKBT ceramics, the microdomain–macrodomain transition occurs at T_{tr}, corresponding to rhombohedral–tetragonal ferroelectric phase transition. And microdomain will separate to form polar micro region at Curie temperature T_m, which is related to ferroelectric–paraelectric phase transition. Zhang Dongjie and Yao Xi reported a new criterion to judge the stability of microdomain[24]:

$$K = \exp\left[-\frac{1}{\delta}\frac{T}{T_m}\right] \tag{7}$$

where K stands for the stability of microdomain. The larger the K value is, the more stability of microdomain is and the more

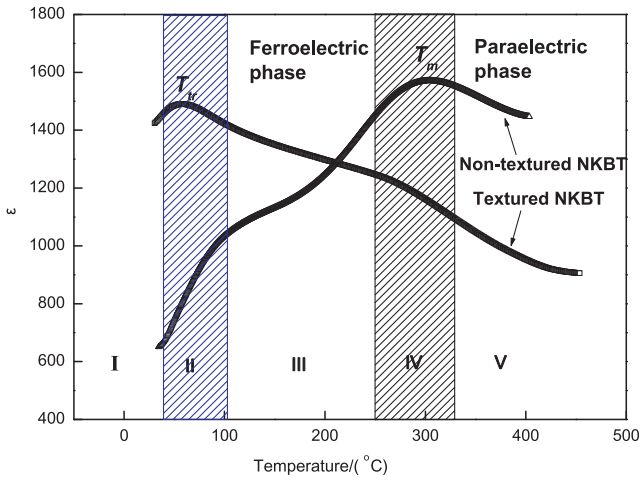

Fig. 10. The sketch map of microdomain–macrodomain transition for non-textured and textured NKBT ceramics. I: Macrodomain region; II: Microdomain + macrodomain; III: Microdomain region; IV: Microdomain + Polar micro region; V: Polar micro region.

energy is needed to the microdomain–macrodomain transition. Thus, the stronger relaxor behavior shows.

Fig. 10 shows the sketch map of microdomain–macrodomain transition for non-textured and textured NKBT ceramics is shown in. There are five parts in Fig. 10. T_{tr} lies in the second part corresponding to microdomain–macrodomain transition. The K value is a criterion signified the stability of microdomain. Here we consider that the macrodomain is a region where microdomain runs in order, and owns nano-size similar to that of the order micro-region with ~90 nanometer in La-doped PMN ceramics.[25]

Fig. 11 shows the K value of textured and non-textured NKBT ceramics at temperature range from 80 °C to 270 °C. The K value of textured NKBT ceramics is smaller than that of the non-textured NKBT ceramics. It indicates that microdomains of the non-textured NKBT ceramics are more stable than those of textured NKBT ceramics. Comparing with the non-textured NKBT ceramics, it is easier for textured NKBT ceramics to

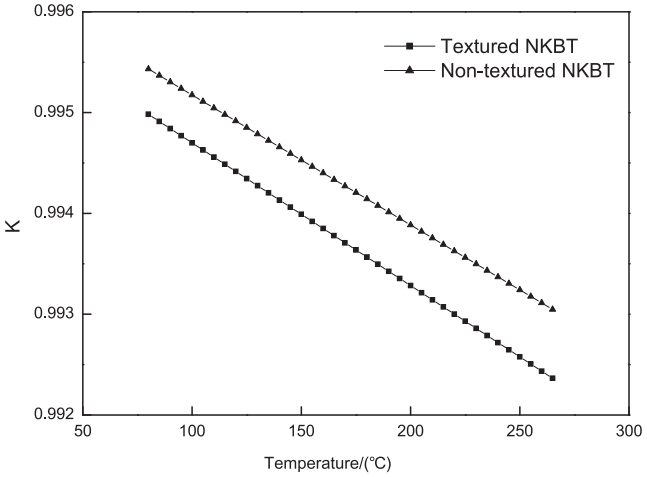

Fig. 11. The microdomain stability of non-textured and textured NKBT ceramics.

take microdomain–macrodomain transition. Furthermore, the volume percentage of microdomain in textured NKBT ceramics is lower than that of non-textured NKBT ceramics. Taking into account of results and factors mentioned above, it can be concluded that the stability of microdomain is the original reason for the dielectric relaxor behavior. The formation of texture will lower the stability of microdomain and make it easy to grow from microdomain to macrodomain, which will weaken the relaxor behavior and raise the dielectric constant at T_{tr}.

Fig. 12 shows the temperature dependence of dielectric properties of NKBT textured ceramics with different soaking times. It is revealed that there are no obviously changes with extending the soaking times. The same trend of diffuse phase transition is observed. The diffuseness of a phase transition can be determined from the modified Curie–Weiss law:[26,27]

$$\frac{1}{\varepsilon} - \frac{1}{\varepsilon_m} = C(T - T_m)^r \tag{8}$$

where ε_m is the maximum value of dielectric constant at the phase transition temperature T_m, γ is the degree of diffuseness

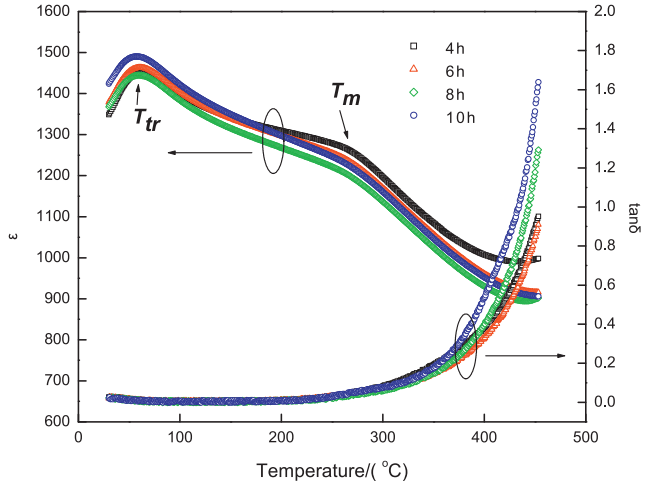

Fig. 12. Temperature dependence of dielectric properties of NKBT textured ceramics with different soaking times.

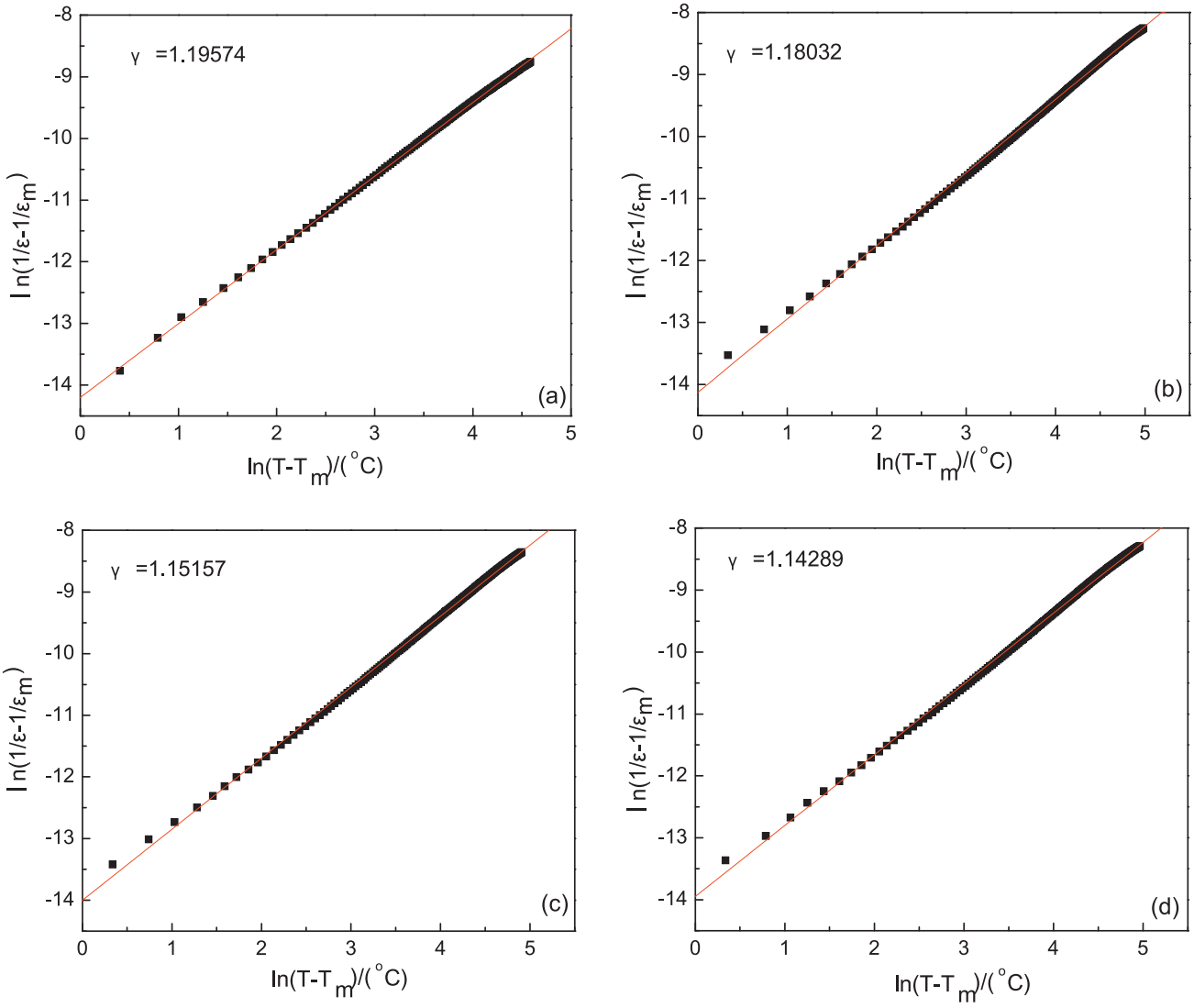

Fig. 13. The diffusion coefficient γ of NKBT textured ceramics with different soaking times: (a) 4 h, (b) 6 h, (c) 8 h and (d) 10 h.

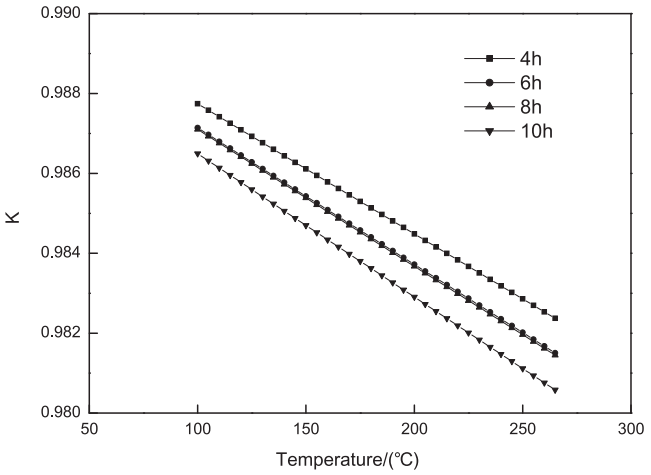

Fig. 14. The microdomain stability of textured NKBT ceramics with different soaking times.

and C is the Curie-like constant. γ can range from 1 for a normal ferroelectrics to 2 for an ideal relaxor ferroelectrics. Eq. (8) can be transformed into Eq. (9) by logarithmizing the two sides:

$$\mathrm{Ln}\left(\frac{1}{\varepsilon}-\frac{1}{\varepsilon_m}\right)=\gamma\,\mathrm{Ln}\,(T-T_m)+\mathrm{Ln}\,C \tag{9}$$

From Eq. (9), $\mathrm{Ln}(1/\varepsilon-1/\varepsilon_m)$ is linearly proportional to $\mathrm{Ln}(T-T_m)$ when ε_m and T_m are determined. The γ value can be acquired from the slope ratio. Fig. 13 shows the function of $\mathrm{Ln}(1/\varepsilon-1/\varepsilon_m)$ versus $\mathrm{Ln}(T-T_m)$. It is obvious that textured NKBT ceramics with different soaking times show a linear relationship of $\mathrm{Ln}(1/\varepsilon-1/\varepsilon_m)$ and $\mathrm{Ln}(T-T_m)$. The γ values were therefore calculated from the experimental data by the least-squared fitting method, respectively. As the soaking time increases, γ decreases from 1.19574 at 4 h to 1.14289 at 10 h. This means that the relaxor characteristic of textured NKBT ceramics would be weakened by increasing soaking times. And this will take the higher dielectric constant. The criterion for the stability of microdomain (K) of textured NKBT ceramics at different soaking times was calculated and shown in Fig. 14. It indicates that the K values decrease with increasing soaking time. Because the degree of orientation increases with soaking times, as discussed above, formation of texture will responsible to weaken relaxor behavior.

4. Conclusions

Textured $0.96(0.8Na_{0.5}Bi_{0.5}TiO_3–0.2\,K_{0.5}Bi_{0.5}TiO_3)–0.04NaNbO_3$ (NKBT) ceramics were fabricated by the RTGG method with plate-like $NaNbO_3$ (NN) template particles. The results show that textured ceramics were successfully obtained with an orientation factor of more than 0.7. NKBT specimens are composed of strip-like grains and equiaxed shaped grains. The textured ceramics have a microstructure with strip-like grains aligned in the direction parallel to the casting plane and exhibit an $\{h\,0\,0\}$ preferred orientation. The degree of grain orientation increases initially, then decreases with increasing sintering temperature, while it is continuously increasing with the soaking time rising to 10 h. A sintering temperature of 1150 °C and soaking time of 10 h are the optimal sintering conditions, where the maximum texture fraction of 0.81 is obtained. Either the NKBT ceramics with random orientation grains or textured NKBT ceramics show evidence of diffuse phase transition and frequency dispersion. However, the dielectric constant at T_{tr} is obviously higher than that of T_m for textured NKBT ceramics. And the relaxor behavior of textured NKBT ceramics would be weakened by increasing soaking times. The results show that the formation of texture is beneficial to microdomain–macrodomain transition and results in the decrease of microdomain, which is the reason why relaxor characteristics weaken and the dielectric constant at T_{tr} raise.

Acknowledgements

This work was supported by Aviation Science Foundation of China and Basic Research Foundation of Northwestern Polytechnical University.

References

1. Takenaka T, Nagata H. Current status and prospects of lead-free piezoelectric ceramics. *J Eur Ceram Soc* 2005;**25**:2693–700.
2. Saito Y, Takao H, Tani T, Nonoyama T, Takatori K, Homma T, et al. Lead-free piezoceramics. *Nature* 2004;**432**(4):84–7.
3. Yang ZP, Hou YT, Liu B, Wei LL. Structure and electrical properties of Nd_2O_3-doped $0.82Bi_{0.5}Na_{0.5}TiO_3$-$0.18Bi_{0.5}K_{0.5}TiO_3$ ceramics. *Ceram Int* 2009;**35**(4):1423–7.
4. Zhang YR, Li JF, Zhang BP, Peng CE. Piezoelectric and ferroelectric properties of Bi-compensated $Na_{0.5}Bi_{0.5}TiO_3$–$K_{0.5}Bi_{0.5}TiO_3$ lead-free piezoelectric ceramics. *J Appl Phys* 2008;**103**, 074109-1-6.
5. Yoo J, Oh DG, Jeong Y, Hong J, Jung M. Dielectric and piezoelectric characteristics of lead-free $(Na_{0.84}K_{0.16})_{0.5}Bi_{0.5}TiO_3$ ceramics substituted with Sr. *Mater Lett* 2004;**58**:3831–5.
6. Li YM, Chen W, Xu Q, Zhou J, Wang Y, Sun HJ. Piezoelectric and dielectric properties of CeO_2-doped $Bi_{0.5}Na_{0.44}K_{0.06}TiO_3$ lead-free ceramics. *Ceram Int* 2007;**33**(1):95–9.
7. Fan G, Lu WZ, Wang XH, Liang F. Morphotropic phase boundary and piezoelectric properties of $Na_{0.5}Bi_{0.5}TiO_3$–$K_{0.5}Bi_{0.5}TiO_3$–$KNbO_3$ lead-free piezoelectric ceramics. *Appl Phys Lett* 2007;**91**, 202908-1-3.
8. Messing GL, Trolier-McKinstry S, Sabolsky EM, Duran C, Kwon S, Brahmaroutu B, et al. Templated grain growth of textured piezoelectric ceramics. *Crit Rev Solid State Mater Sci* 2004;**29**:45–96.
9. Yilmaz H, Trolier-McKinstry S, Messing GL. (Reactive) Templated grain growth of textured sodium bismuth titanate ($Na_{1/2}Bi_{1/2}TiO_3$–$BaTiO_3$) ceramics-II dielectric and piezoelectric properties. *J Electroceram* 2003;**11**:217–26.
10. West DL, Payne DA. Microstructure development in reactive-templated grain growth of $Bi_{1/2}Na_{1/2}TiO_3$-based ceramics: template and formulation effects. *J Am Ceram Soc* 2003;**86**(5):769–74.
11. Fuse K, Kimura T. Effect of particle sizes of starting materials on microstructure development in textured $Bi_{0.5}(Na_{0.5}K_{0.5})_{0.5}TiO_3$. *J Am Ceram Soc* 2006;**89**(6):1957–64.
12. Gao F, Hong RZ, Liu J, Yao YH, Tian CS. Effect of different templates on microstructure of textured $Na_{0.5}Bi_{0.5}TiO_3$–$BaTiO_3$ ceramics with RTGG method. *J Eur Ceram Soc* 2008;**28**(10):2063–70.
13. Hong SH, Trolier-McKinstry S, Messing GL. Dielectric and electromechanical properties of textured niobium-doped bismuth titanate ceramics. *J Am Ceram Soc* 2000;**83**(1):113–8.

14. Sato T, Yoshida Y, Kimura T. Preparation of ⟨1 1 0⟩-textured $BaTiO_3$ ceramics by the reactive-templated grain growth method using needlelike TiO_2 particles. *J Am Ceram Soc* 2007;**90**(9):3005–8.
15. Shoji T, Fuse K, Kimura T. Mechanism of texture development in $Bi_{0.5}(Na,K)_{0.5}TiO_3$ prepared by the templated grain growth process. *J Am Ceram Soc* 2009;**92**(S1):S140–5.
16. Motohashi T, Kimura T. Development of texture in $Bi_{0.5}Na_{0.5}TiO_3$ prepared by reactive-templated grain growth process. *J Eur Ceram Soc* 2007;**27**:3633–6.
17. Konieczny K. Pyroelectric and dielectric study of $NaNbO_3$ single crystals. *Mater Sci Eng B* 1999;**60**:124–7.
18. Hong RZ. Preparation and properties of textured NKBT-based lead-free piezoelectric ceramics. *Thesis for Master Degree of Northwestern Polytechnical University*; 2009.
19. Chang YF, Yang ZP, Chao XL, Liu ZH, Wang ZL. Synthesis and morphology of anisotropic $NaNbO_3$ seed crystals. *Mater Chem Phys* 2008;**111**:195–200.
20. Gao F, Hong RZ, Liu J, Yao YH, Tian CS. Grain growth kinetics of textured $0.92Na_{0.5}Bi_{0.5}TiO_3$–$0.08BaTiO_3$ ceramics by tape casting with $Bi_{2.5}Na_{3.5}Nb_5O_{18}$ templates. *J Electroceram* 2010;**24**(3):145–52.
21. West DL, Payne DA. Reactive-templated grain growth of $Bi_{1/2}(Na,K)_{1/2}TiO_3$: effects of formulation on texture development. *J Am Ceram Soc* 2003;**86**(7):1132–7.
22. Cross LE. Relaxor ferroelectrics. *Ferroelectrics* 1987;**76**:241–67.
23. Yao X, Chen ZL, Cross LE. Polarization and depolarization behavior of hot pressed lead lanthanum zirconate titanate ceramics. *J Appl Phys* 1983;**54**(6):3399–403.
24. Zhang DJ, Yao X. Dynamics on microdomain–macrodomain transition of relaxor ferroelectrics. *Acta Phys Chim Sin* 2004;**20**(7):712–6.
25. Chen J, Chan HM, Harmer MP. Ordering structure and dielectric properties of undoped and La/Na-doped $Pb(Mg_{1/3}Nb_{2/3})O_3$. *J Am Ceram Soc* 1989;**72**(4):593–8.
26. Uchino K, Nomura S. Critical exponents of the dielectric constants in diffused phase transition crystals. *Ferroelectrics Lett Sec* 1982;**44**(1):55–61.
27. Li YM, Chen W, Zhou J, Xu Q, Sun HJ, Liao MS. Dielectric and ferroelectric properties of lead-free $Na_{0.5}Bi_{0.5}TiO_3$-$K_{0.5}Bi_{0.5}TiO_3$ ferroelectric ceramics. *Ceram Int* 2005;**31**:139–42.